
**MAGNETISM
AND FERROELECTRICITY**

Magnetoresistance and Electrical Conductivity of Manganite Bicrystal Contacts

I. V. Borisenko and G. A. Ovsyannikov

*Institute of Radio Engineering and Electronics, Russian Academy of Sciences,
ul. Mokhovaya 18, Moscow, 103907 Russia*

e-mail: iboris@hitech.cplire.ru

Received March 24, 2008

Abstract—Magnetic bicrystal contacts in epitaxial films of manganite $\text{La}_{0.67}\text{Ca}_{0.33}\text{MnO}_3$ prepared on bicrystal substrates with a misorientation of the $\text{NdGaO}_3(110)$ basal planes rotated through an angle of $\pm 14^\circ$ around the bicrystal boundary line were studied. The temperature dependence of the contact electrical resistance was studied, and the magnetoresistance was measured in fields of up to 1.5 kOe. It is shown that the suppression of ferromagnetic correlations near the boundary leads to the formation of a layer having a substantially lower Curie temperature. Magnetoresistance of 150%, which is record-breaking for bicrystal contacts, was measured at $T = 4.2$ K in a weak magnetic field of about 500 Oe and at a characteristic electrical resistance of the boundary of $3 \times 10^{-6} \Omega \text{ cm}^2$. It is found that slight orthorhombic distortions of a $\text{La}_{0.67}\text{Ca}_{0.33}\text{MnO}_3$ film due to a lattice mismatch with the $\text{NdGaO}_3(110)$ substrate crystal structure lead to the formation of biaxial magnetic anisotropy in the $\text{La}_{0.67}\text{Ca}_{0.33}\text{MnO}_3$ film.

PACS numbers: 75.47.-m, 85.75.-d

DOI: 10.1134/S1063783409020176

1. INTRODUCTION

Magnetic contacts are main elements of spintronic devices in which manipulations are performed with spin states of a system rather than with its charge states [1]. The most attractive materials for applications in magnetic contacts are ferromagnets with a carrier spin polarization close to 100%. For such materials used in magnetic contacts, one can expect record-breaking magnetoresistance and the strongest effects due to a significant spin injection. As shown earlier (see, e.g., [2]), doped manganites of the $\text{La}_{1-x}\text{A}_x\text{MnO}_3$ type ($A = \text{Sr, Ca, Ba, etc.}$) with an optimal doping level $x \approx 0.33$ are ferromagnetic materials with a high carrier polarization close to 100%. In the ferromagnetic state, these materials are semimetals in which only one spin subband exhibits a nonzero density of states at the Fermi level. As a result, the electrical resistance of a contact between two manganites is mainly determined by the mutual orientation of their magnetizations. However, the fabrication of magnetic contacts from manganites is hampered by their high sensitivity to both the degradation of the chemical composition and the electronic state near the interface, which, in turn, decreases the effective spin polarization of the current passed through the contact. One way to produce magnetic contacts with high-quality boundaries is the use of a bicrystal boundary in a thin epitaxial film grown on a bicrystal substrate. In recent years, several publications have been devoted to investigating magnetic contacts at bicrystal

boundaries obtained in epitaxial films grown on bicrystal SrTiO_3 and LaAlO_3 substrates with misorientation of the crystallographic axes around the [001] direction [3–5]. The contacts obtained exhibited comparatively low magnetoresistance (30–40%) and high ohmic resistance (10^{-5} – $10^{-2} \Omega \text{ cm}^2$). The studies of metal oxide superconductor bicrystal boundaries conducted in [6, 7] showed that the misorientation of the basal planes around the bicrystal-boundary line substantially improves the boundary microstructure, decreases the characteristic resistance of the boundary, and increases the characteristic Josephson voltage. This type of bicrystal boundary possesses an essentially lower dislocation concentration in the boundary plane and exhibits a more qualitative morphology of the boundaries [7].

The aim of this work is to prepare magnetic $\text{La}_{0.67}\text{Ca}_{0.33}\text{MnO}_3$ contacts on a bicrystal $\text{NdGaO}_3(110)$ substrate with misorientation of the basal planes around the bicrystal boundary and to study their transport properties, the mechanisms of magnetization reversal, and magnetoresistance.

2. EXPERIMENTAL

50-nm-thick $\text{La}_{0.67}\text{Ca}_{0.33}\text{MnO}_3$ (LCMO) epitaxial films were grown by the laser ablation method on $\text{NdGaO}_3(110)$ (NGO) bicrystal substrates with $\pm 14^\circ$ misorientation of their axes about the $[1\bar{1}0]$ direction (Fig. 1). For LCMO grown on NGO substrates, the fol-

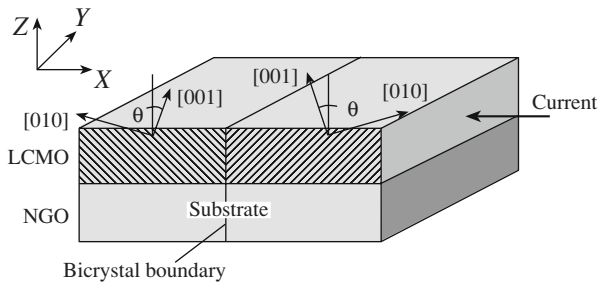


Fig. 1. Bicrystal boundary in an NGO substrate and an LCMO film (schematic). The X, Y, and Z axes coincide with the directions along which an external magnetic field was applied when measuring the magnetoresistance. The crystallographic directions in the LCMO film are indicated by the arrow pairs. The external current is passed in the substrate plane perpendicular to the boundary.

lowing epitaxial relations were satisfied: $\text{LCMO}(001) \parallel \text{NGO}(110)$ and $\text{LCMO}[100] \parallel \text{NGO}[1\bar{1}0]$. The LCMO pseudocubic lattice parameter $a_L = 3.858 \text{ \AA}$, and the NGO(110) lattice parameters (orthorhombic unit cell with $a = 5.426 \text{ \AA}$, $b = 5.502 \text{ \AA}$, and $c = 7.706 \text{ \AA}$) along the [001] and $[1\bar{1}0]$ directions are $a_N = 3.853 \text{ \AA}$ and $b_N = 3.863 \text{ \AA}$, respectively [8]. Since $a_N < a_L < b_N$, stresses of opposite polarity arise in an LCMO film, namely, compressive stresses along $\text{NGO}[001]$ and tensile stresses along $\text{NGO}[1\bar{1}0]$.

Films were grown by laser ablation in an oxygen atmosphere at a pressure $P = 0.2 \text{ mbar}$ at a substrate temperature $T = 750^\circ\text{C}$ with subsequent annealing in oxygen at a pressure of 1 bar. In a film, 7- μm -wide bridges intersecting the bicrystal boundary were formed by ion-beam etching using a photoresist mask. All electrophysical measurements were carried out by the four-probe method using platinum contact areas deposited by rf sputtering through a metallic mask. During epitaxial growth, the bicrystal-substrate crystalline structure is reproduced in an LCMO film and a bicrystal boundary is formed in the film. The translation symmetry is broken at the boundary. As a result, the electronic state is transformed, which, in turn, leads in manganites to the occurrence of a thin separation layer with high resistivity (Fig. 1).

3. EXPERIMENTAL RESULTS AND DISCUSSION

Figure 2 presents the temperature dependence of the electrical resistance of an LCMO bridge intersecting the bicrystal boundary (curve 3) measured on cooling in a zero magnetic field. In order to determine the contribution of the electrical resistance of the “banks” to the total resistance, we measured the resistance of an LCMO bridge-shaped film with the same geometric sizes not intersecting the boundary (curve 2). The electrical resistance of the bicrystal boundary (curve 3) was

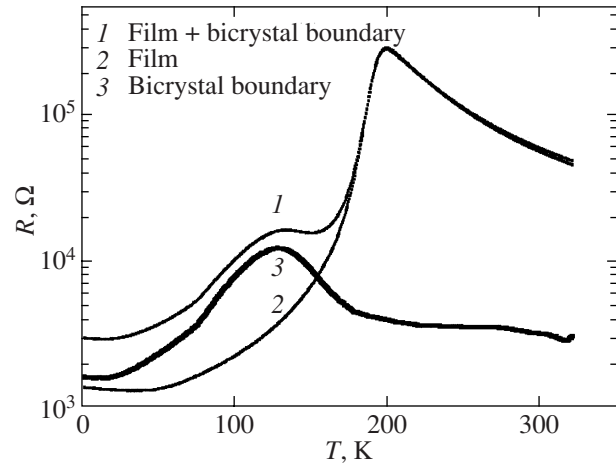


Fig. 2. Temperature dependence of the electrical resistance of the bicrystal boundary in an LCMO film (curve 3) obtained from measurements of the resistances of (1) the total structure and (2) the leads. The measurements were performed in a weak magnetic field (on the order of the Earth magnetic field).

obtained by subtracting the resistance of the film (curve 2) from the total resistance of the sample (curve 1). The transition to the ferromagnetic state in manganites in the vicinity of the Curie temperature T_C is always accompanied by an insulator–metal transition, which manifests itself as a peak at a temperature T_p in the temperature dependence of the resistance. Usually, T_p is several degrees lower than T_C [9, 10]. The Curie temperature of bulk single-crystal LCMO samples is $T_C \approx 250 \text{ K}$, while T_p of a film is 210 K, as seen from Fig. 2. From the temperature dependence of the resistance of the bicrystal boundary itself, it follows that, near the boundary, T_p is suppressed to 130 K in comparison to T_p in the banks (210 K). A high characteristic resistance of the boundary $RS = 3 \times 10^{-6} \Omega \text{ cm}^2$ at $T = 4.2 \text{ K}$ (where R and S are the resistance and the area of the bicrystal contact, respectively) indicates the existence of a barrier layer with a transparency of 10^{-3} – 10^{-4} , whose appearance is most likely caused by a larger depletion of the charge density to a subcritical value at which a nonferromagnetic insulating state is formed.

The dependence of the electrical resistance on magnetic field was measured at 4.2 K in fields of up to 1.5 kOe for three mutually perpendicular directions of the magnetic field: along the normal to the substrate plane (axis Z), along the bicrystal-boundary line (axis Y), and along the normal to the bicrystal-boundary plane (axis X, Fig. 1). The relative magnetoresistance (MR) was calculated from the formula

$$\text{MR} = (R^{\text{AP}} - R^{\text{P}})/R^{\text{P}}, \quad (1)$$

where R^{AP} and R^{P} are the electrical resistances measured at low voltages for the antiparallel and parallel mutual orientations of the magnetizations in the contact

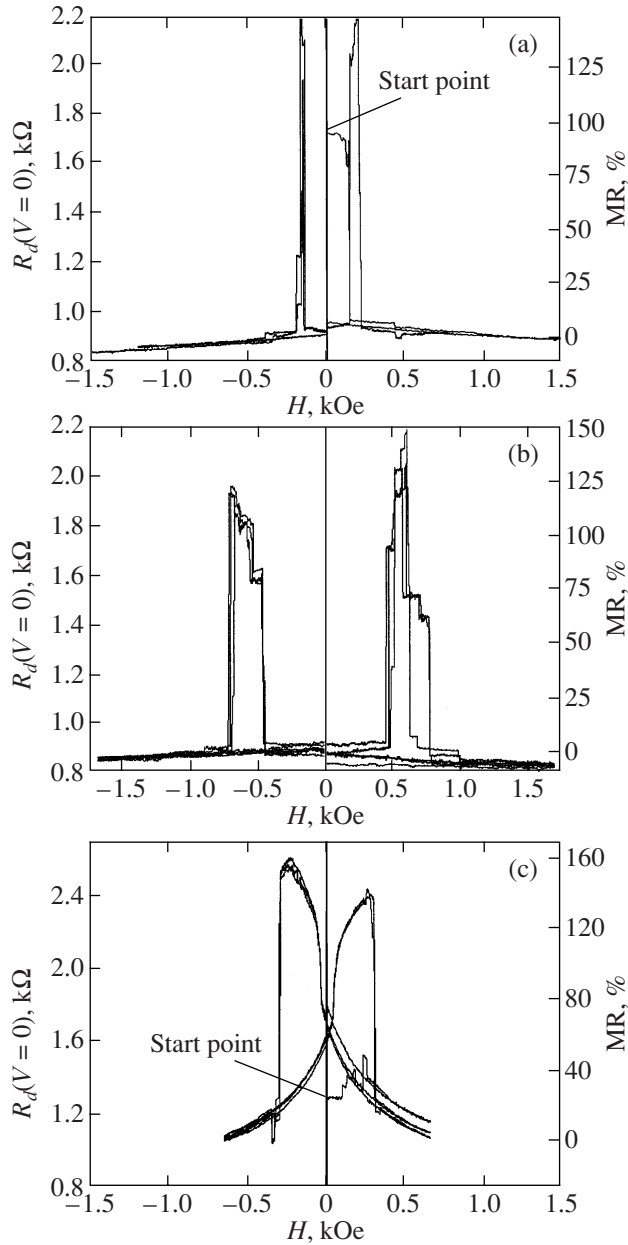


Fig. 3. Magnetoresistance of a bicrystal boundary in an LCMO film measured at $T = 4.2$ K as a function of external magnetic field applied along (a) the Y, (b) Z, and (c) X axes. The differential resistance of the bicrystal boundary at a zero stress (on the left) and its variation in percent (on the right) are shown.

banks, respectively. The maximum magnetoresistance was nearly 150% (Figs. 3a–3c), which substantially exceeds the values of about 30% found earlier on bicrystal contacts with the axes rotated in the substrate plane [3–5]. The magnetization reversal in magnetic fields applied along the Y and Z axes is accompanied by a jump in resistance within relatively narrow magnetic-field ranges 75 and 300 Oe wide, respectively (Figs. 3a and 3b), which demonstrates a sharp reorientation of

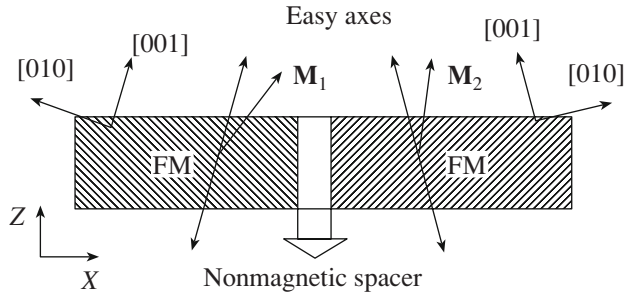


Fig. 4. Model used to describe the magnetization reversal in a bicrystal boundary (schematic). The arrows show the crystallographic directions in the LCMO film, the easy magnetization axes oriented symmetrically with respect to the contact plane, and the magnetic moment vectors \mathbf{M}_1 and \mathbf{M}_2 .

the magnetization in the film near the bicrystal boundary. In magnetic fields applied along the X axis, the dependence of the electrical resistance on magnetic field is smooth, which corresponds to the coherent magnetization rotation in the contact banks (Fig. 3c).

We analyzed the processes of magnetization reversal in a bicrystal contact using a model in which two ferromagnets rectangular in shape with equal uniform magnetization are separated by a thin layer of a nonmagnetic material. The contact banks interact through their magnetostatic extraneous fields. The ferromagnets have first-order easy-axis magnetic anisotropy and a mirror-symmetric arrangement of the axes with respect to the bicrystal-boundary plane. In simulations, the adjustable parameters are the magnetizations of the ferromagnets, the magnetic anisotropy field, and the orientation of the easy-magnetization axes (Fig. 4). To calculate the magnetoresistance, we used a formula additively including the contact conductance independent of the mutual orientation of the magnetizations

$$G(H) = G_0 + G_M(1 + \mathbf{m}_1 \cdot \mathbf{m}_2), \quad (2)$$

where G_0 is the field-independent part of the total contact conductance, G_M is the amplitude of the field-dependent part of the contact conductance, and $\mathbf{m}_i = \mathbf{M}_i/|\mathbf{M}_i|$ are the magnetization unit vectors of the contact banks entering into Eq. (2) through their scalar product.

The results of the simulation for magnetic fields applied along the Z and X axes are presented in Figs. 5a and 5b. The magnetization obtained for an LCMO film (400 emu/cm^3) by fitting the experimental data agrees well with that of epitaxial films measured by a SQUID magnetometer [11]. The best fit to the experimental data is obtained when the easy magnetization axis is deviated from the normal to the film surface through angles of $\pm 14^\circ$ and coincides with the [001] direction of the LCMO film. Moreover, the measurement of the magnetoresistance along the Y axis shows that there is another easy magnetization axis coinciding with the

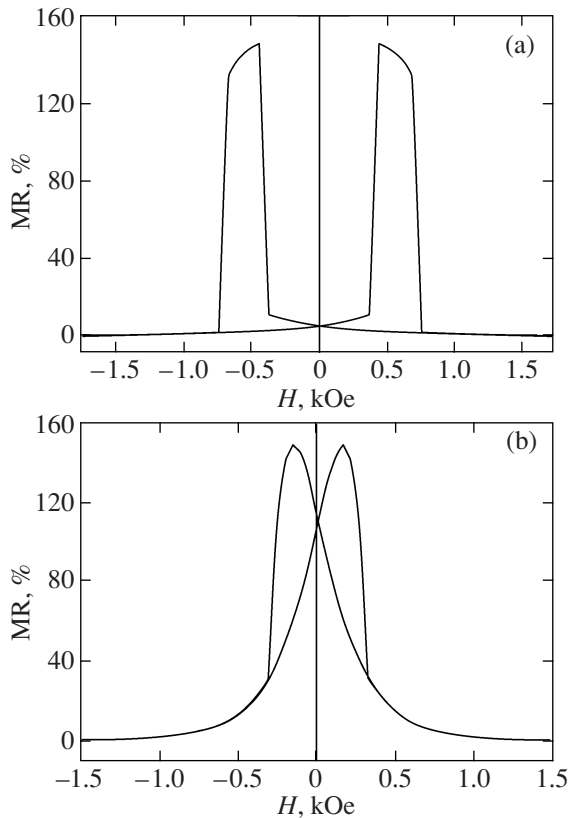


Fig. 5. Field dependences of the magnetoresistance obtained from simulating the magnetization reversal in magnetic fields directed along (a) the Z and (b) X axes.

[100] direction in the LCMO. The study of the influence of stresses on the magnetic anisotropy in manganite films (see, e.g., [5]) grown on SrTiO_3 and LaAlO_3 substrates having cubic lattices showed that the compressive stress in the (001) plane causes the appearance of an easy magnetization axis along the LCMO[001] direction (for LaAlO_3) and that the tensile stress in the LCMO(001) plane creates in-plane easy magnetization axes along the [110] and $[1\bar{1}0]$ directions (for SrTiO_3). Although the effect of stresses on the magnetic anisotropy of LCMO films on NGO substrates has not been studied, we can conclude, based on the data for SrTiO_3 and LaAlO_3 substrates, that tensile stresses in the direction LCMO[100] \parallel NGO $[1\bar{1}0]$ and compressive stresses in the direction LCMO[010] \parallel NGO[001] create easy magnetization axes along the LCMO[100] and LCMO[001] directions.

In the experiment with magnetic fields applied along the Z and Y axes, the switching of the contact resistance between the high- and low-ohmic states occurs in steps and sometimes is not reproduced during multiple cycling. Therefore, we can conclude that an LCMO film near the boundary is in a multidomain state and its magnetization reversal occurs either through the reversal of a domain magnetization or through a step-

wise displacement of a domain boundary. From comparing the width (in magnetic field) of each magnetization reversal step with the total width of the resistance peak, we can qualitatively estimate the magnetic domain size. For magnetic fields directed along the Z axis, the total peak width is 300 Oe and the mean step width is nearly 30 Oe. Therefore, for a contact width of $7\ \mu\text{m}$, the domain dimension along the bicrystal boundary is $0.7\ \mu\text{m}$. Due to the formation of a multidomain structure in a manganite film near the boundary in the high-ohmic state, the magnetoresistance averaged over the transition width can be substantially lower than the maximum attainable local value that could be observed, e.g., in junctions with a submicron width.

4. CONCLUSIONS

We have shown experimentally that magnetic contacts prepared on a bicrystal substrate with the inclined basal planes exhibit high magnetoresistance of up to 150% in magnetic fields of up to 1 kOe. However, the prepared contacts have a fairly high characteristic electrical resistance of the bicrystal boundary, which hampers the study of their dynamic properties and the effects of the high-current injection of spin-polarized carriers. It is likely that the use of bicrystal substrates with small misorientation angles could permit one to solve this problem. Based on the established dependence of the magnetic anisotropy of manganite films on the substrate crystallographic orientation and on the relationship between the lattice parameters of the film and the substrate, one can create magnetically sensitive elements with predetermined properties by properly choosing these parameters.

ACKNOWLEDGMENTS

We are grateful to V.V. Demidov, D. Winkler, T. Claeson, A. Klimov, K.I. Konstantinyan, I.M. Kotelianskiĭ, and A.V. Shadrin for useful discussion of the results of the study and their assistance in performing the study.

This work was supported by the Department of Physical Sciences of the Russian Academy of Sciences, the Ministry of Education and Science of the Russian Federation, a program of the European Union (project NMP3-CT-2006-033191), the AQDJJ and THIOX programs of the European Scientific Foundation, and the International Scientific and Technical Center (project 3743).

REFERENCES

1. I. Žutic, *Rev. Mod. Phys.* **76**, 323 (2004).
2. M. Bowen, M. Bides, A. Barthél my, J.-P. Contour, A. Anane, Y. Lema tre, and A. Fert, *Appl. Phys. Lett.* **82**, 233 (2003).

3. N. D. Mathur, G. Burnell, S. P. Isaac, T. J. Jackson, B.-S. Teo, J. L. MacManus-Driscoll, L. F. Cohen, J. E. Evetts, and M. G. Blamire, *Nature (London)* **387**, 266 (1997).
4. J. Klein, C. Hofener, S. Uhlenbruck, L. Alff, B. Buchner, and R. Gross, *Europhys. Lett.* **47**, 371 (1999).
5. R. Gunnarsson and M. Hanson, *Phys. Rev. B: Condens. Matter* **73**, 014 435 (2006).
6. I. V. Borisenko, I. M. Kotelyanski, A. V. Shadrin, P. V. Komissinski, and G. A. Ovsyannikov, *IEEE Trans. Appl. Supercond.* **15**, 165 (2005).
7. Y. Y. Divin, U. Poppe, C. L. Jia, P. M. Shadrin, and K. Urban, *Physica C (Amsterdam)* **372–376**, 115 (2002).
8. Yu. A. Boikov and V. A. Danilov, *Pis'ma Zh. Tekh. Fiz.* **31** (14), 50 (2005) [*Tech. Phys. Lett.* **31** (7), 605 (2005)].
9. Yu. A. Izyumov and Yu. N. Skryabin, *Usp. Fiz. Nauk* **171** (2), 121 (2001) [*Phys.—Usp.* **44** (2), 109 (2001)].
10. Y. P. Lee, S. Y. Park, Y. H. Hyun, J. B. Kim, V. G. Prokhorov, V. A. Komashko, and V. L. Svetchnikov, *Phys. Rev. B: Condens. Matter* **73**, 224 413 (2006).
11. T. K. Nath, R. A. Rao, D. Lavric, C. B. Eom, L. Wu, and F. Tsui, *Appl. Phys. Lett.* **74**, 1615 (1999).

Translated by Yu. Ryzhkov